Constitutive release of CPS1 in bile and its role as a protective cytokine during acute liver injury

Min-Jung Park[a,1], Louis G. D'Alecy[a], Michelle A. Anderson[b], Venkatesha Basrur[c], Yongjia Feng[a], Graham F. Brady[a,b], Dong-il Kim[d], Jun Wu[a,e], Alexey I. Nesvizhskii[c], Joerg Lahann[f,g], Nicholas W. Lukacs[c], Robert J. Fontana[b], and M. Bishr Omary[a,b,h,1]

[a]Department of Molecular and Integrative Physiology, University of Michigan Medical School, Ann Arbor, MI 48109; [b]Department of Internal Medicine, Division of Gastroenterology and Hepatology, University of Michigan Medical School, Ann Arbor, MI 48109; [c]Department of Pathology, University of Michigan Medical School, Ann Arbor, MI 48109; [d]Department of Physiology, College of Veterinary Medicine, Chonnam National University, 61186 Gwangju, Republic of Korea; [e]Life Sciences Institute, University of Michigan, Ann Arbor, MI 48109; [f]Biointerfaces Institute, College of Engineering, University of Michigan, Ann Arbor, MI 48109; [g]Department of Biomedical Engineering, University of Michigan, Ann Arbor, MI 48109; and [h]Cell Biology, Faculty of Science and Technology, Åbo Akademi University, 20500 Turku, Finland

Edited by Michael Karin, University of California, San Diego School of Medicine, La Jolla, CA, and approved March 14, 2019 (received for review January 3, 2019)

Carbamoyl phosphate synthetase-1 (CPS1) is the major mitochondrial urea cycle enzyme in hepatocytes. It is released into mouse and human blood during acute liver injury, where is has a short half-life. The function of CPS1 in blood and the reason for its short half-life in serum are unknown. We show that CPS1 is released normally into mouse and human bile, and pathologically into blood during acute liver injury. Other cytoplasmic and mitochondrial urea cycle enzymes are also found in normal mouse bile. Serum, bile, and purified CPS1 manifest sedimentation properties that overlap with extracellular vesicles, due to the propensity of CPS1 to aggregate despite being released primarily as a soluble protein. During liver injury, CPS1 in blood is rapidly sequestered by monocytes, leading to monocyte M2-polarization and homing to the liver independent of its enzyme activity. Recombinant CPS1 (rCPS1), but not control r-transferrin, increases hepatic macrophage numbers and phagocytic activity. Notably, rCPS1 does not activate hepatic macrophages directly; rather, it activates bone marrow and circulating monocytes that then home to the liver. rCPS1 administration prevents mouse liver damage induced by Fas ligand or acetaminophen, but this protection is absent in macrophage-deficient mice. Moreover, rCPS1 protects from acetaminophen-induced liver injury even when given therapeutically after injury induction. In summary, CPS1 is normally found in bile but is released by hepatocytes into blood upon liver damage. We demonstrate a nonenzymatic function of CPS1 as an antiinflammatory protective cytokine during acute liver injury.

mitochondria | bile proteome | macrophage polarization | acetaminophen | Fas ligand

Acute liver failure is a life-threatening illness defined by rapid deterioration in liver function frequently resulting in diverse clinical features, including hepatic encephalopathy and bleeding diathesis. Approximately 2,000 people develop acute liver failure annually in the United States, and more than half of the cases are caused by drug-induced liver injury, particularly overdoses with acetaminophen (APAP), or other etiologies, including viral infection, alcoholic hepatitis, other drug reactions, and hepatic ischemia (1, 2).

Several proteins, called alarmins or damage-associated molecular patterns (DAMPs), are released during liver and other tissue injury and are involved in disease progression. For example, high-mobility group box-1 (HMGB1) is the prototypic DAMP protein released during diverse context of damage (3–6). HMGB1 functions as a DNA chaperone in the nucleus; however, upon release, it triggers the secretion of proinflammatory cytokines through binding to Toll-like receptor-4 (TLR4) or the receptor for advanced glycation end products (RAGE) (7). Inner mitochondrial membrane cytochrome *c* is another protein found in the extracellular space under pathological condition with a potential role as a DAMP (8, 9). Moreover, DNA, RNA, and mitochondrial DNA are also considered as DAMPs (10, 11). Therefore, high levels of these molecules in serum could represent altered homeostasis, but the specific injured tissue may be difficult to ascertain because of their overall broad tissue distribution.

The mitochondrial enzyme carbamoyl phosphate synthetase-1 (CPS1) is released into the bloodstream during acute liver injury in humans and mice (12). CPS1 is the most abundant mitochondrial matrix protein with long half-life (7.7 d) in hepatocytes (13, 14). It is a 160-kDa protein, composed of multidomains catalyzing synthesis of carbamoyl phosphate from ammonia and bicarbonate, which is important to remove excessive ammonia from portal blood in the first step of the urea cycle (15, 16). CPS1 expression is highly enriched in liver parenchyma, with much lower expression in the small intestine and even lower

Significance

The mitochondrial matrix and urea cycle enzyme carbamoyl phosphate synthetase-1 (CPS1) is released from injured hepatocytes and has a short half-life, but the significance for both is unknown. We show that CPS1 is normally found in bile but is released into blood during liver injury. The short half-life of CPS1 is due to its rapid uptake by monocytes, which then become antiinflammatory, independent of CPS1 enzyme activity, and home to the liver. Notably, recombinant CPS1 blocks liver injury in two experimental mouse models and accelerates recovery even when administered after the injury. Our findings highlight a new nonenzymatic function of CPS1 as an antiinflammatory cytokine and provide a mechanism for its protective action, with exciting therapeutic implications in the liver.

Author contributions: M.-J.P. and M.B.O. designed research; M.-J.P., L.G.D., M.A.A., Y.F., G.F.B., and D.-i.K. performed the experiments; M.-J.P., L.G.D., M.A.A., V.B., Y.F., G.F.B., D.-i.K., J.W., A.I.N., J.L., N.W.L., R.J.F., and M.B.O. analyzed data; L.G.D. and M.A.A. collected the bile samples; V.B. and A.I.N. performed the LC/MS-MS; and M.-J.P. and M.B.O. wrote the paper.

Conflict of interest statement: M.J.P. and M.B.O. are part of a provisional patent application sponsored by the University of Michigan related to the potential use of CPS1 to treat select types of human liver disease. Neither author has received any financial gain related to this work.

This article is a PNAS Direct Submission.

Data deposition: The data reported in this paper have been deposited in the Gene Expression Omnibus (GEO) database, https://www.ncbi.nlm.nih.gov/geo (accession no. GSE122879).

[1]To whom correspondence may be addressed. Email: gguger1@gmail.com or mbishr@umich.edu.

This article contains supporting information online at www.pnas.org/lookup/suppl/doi:10.1073/pnas.1822173116/-/DCSupplemental.

Published online April 12, 2019.

levels in other tissues. CPS1 is a potential prognostic serum marker of liver injury because of its preferential expression in the liver, its short serum half-life compared with other liver enzymes, such as alanine aminotransferase, and its abundance (12, 17). The CPS1 level, which is barely detectable in normal lung, correlates negatively with survival of patients harboring nonsmall cell lung cancer. This observation occurs possibly via increasing the cellular pyrimidine pool (18), although the role of CPS1 enzyme activity and the mechanism of its effect are not clear.

We hypothesized that the short half-life of CPS1 is due to degradation in serum, or to uptake by leukocytes or endothelial cells. Our findings show that CPS1 is released normally into mouse and human bile as a soluble but aggregation-prone protein, but becomes released into serum under pathologic conditions, where it is taken up by monocytes/macrophages (Mϕ) and leads to M2 polarization independent of its enzyme activity. Recombinant (r)CPS1 leads to M2 polarization of Mϕ and is able to both prevent and protect from liver injury through Mϕ. Our findings indicate that the urea cycle enzyme CPS1 functions nonenzymatically as an antiinflammatory cytokine that protects from acute liver injury.

Results

CPS1 Is Released as a Soluble Multimeric Protein. We previously reported CPS1 release into serum during liver injury (12), and others found (using proteomic profiling) CPS1 in the extracellular vesicle (EVs) fraction secreted by rat primary hepatocytes (19). Nanoparticle tracking analysis (NTA), performed with culture media of mouse primary hepatocytes, showed that hepatocytes normally release EVs sized 102.8 ± 1.9 nm on average, with a slight increase in size after incubation with Fas ligand (FL) and subsequent injury (Fig. 1*A*). The mechanism of CPS1 release during liver injury is unknown and CPS1 gene sequence does not contain a leader signal peptide for the classic endoplasmic reticulum–Golgi-dependent secretory pathway. Indeed, inhibitors of classic exocytosis (brefeldin A, Exo1) did not block its release (*SI Appendix*, Fig. S1*A*). CPS1 levels increased in hepatocyte culture media after incubation with FL along with DAMPs—such as HMGB1, lactate dehydrogenase (LDH), and cytochrome *c* (Fig. 1*B*)—but CPS1 was the major protein detected in the EV fraction collected by ultracentrifugation (100,000 × *g* pellet) of the culture media (Fig. 1*B*), consistent with the previous report (19). CPS1 release becomes enhanced not only by FL but also after incubation with rotenone or glucose oxidase, which increase intracellular oxidative stress and result in distinct release patterns for HMGB1, LDH, or other mitochondrial proteins, such as cytochrome *c* and pyruvate dehydrogenase (PDH) (*SI Appendix*, Fig. S1*B*).

To examine the size of CPS1-containing EVs, culture media of hepatocytes or sera from mice given FL or APAP was pelleted at 10,000/20,000/100,000 × *g* serially to enrich for apoptotic bodies, microvesicles, or exosomes, respectively. Unlike HMGB1, LDH, and cytochrome *c*, which were detected exclusively in the supernatant of FL-treated cells, CPS1 copartitioned with the exosome-enriched fraction (100,000 × *g*) and the supernatant ex vivo (*SI Appendix*, Fig. S1*C*) and in vivo (Fig. 1*C*). Notably, none of these proteins was found in serum of healthy mice. Another mitochondrial matrix protein (PDH) and an outer-membrane protein (Tom20) were observed in mouse sera independent of liver injury, but increased in the exosome fraction during liver injury (Fig. 1*C*). The exosome markers CD9 and TSG101 partitioned with the pellet as expected, but were also in the supernatant, suggesting leakage during fractionation or possibly being components of smaller vesicles that are not sedimented by 100,000 × *g* centrifugation. However, incubation of hepatocytes with potential inhibitors for exosome secretion (GW4869 and amiloride) did not alter CPS1 release (*SI Appendix*, Fig. S1*D*), nor did treatment with fausdil or Y-27632 [which inhibit Rho-associated, coiled-coil containing protein kinase (ROCK) signaling and modulate plasma membrane shedding] block CPS1 exocytosis (*SI Appendix*, Fig. S1*E*). NTA analysis of culture media from hepatocytes transduced with CPS1-GFP showed that most of the CPS1-containing GFP^+ particles were smaller than 40 nm (mode: 35.3 ± 0.6 nm) (Fig. 1*D*), which is similar to the smallest size of the expected exosome size (20, 21). However, sucrose gradient separation showed that CPS1 was broadly detected in most of the fractions from the 100,000 × *g* pellet isolated from hepatocyte culture media, whereas the exosome markers CD9, TSG101, Flotillin1, and Alix were exclusively in fractions #7–9 (Fig. 1*E*). In addition, sucrose gradient centrifugation of mice sera showed that CPS1 in the supernatant after 100,000 × *g* spin sedimented in fraction #7–10 (*SI Appendix*, Fig. S2*A*), thereby indicating that even soluble CPS1 forms multimers that cosediment with EVs. Supporting this, electron microscopy of immunogold staining of CPS1 in the 100,000 × *g* pellet of mouse serum showed immune reactivity with aggregate-like structures (*SI Appendix*, Fig. S2*B*). Moreover, sucrose gradient separation of purified recombinant CPS1 (rCPS1) that we generated (*SI Appendix*, Fig. S3*A*) showed a broad distribution consistent with formation of CPS1 multimers (Fig. 1*F*). Collectively, these data are consistent with CPS1 release from hepatocytes as a soluble protein that spontaneously forms multimers, with sedimentation properties that overlap with EVs.

CPS1 Is Found in Normal Mouse and Human Bile. CPS1 is not observed in serum of healthy mice (Fig. 1*C*), but is readily detected in hepatocyte culture media in the absence of insults unlike, HMGB1 and LDH (Figs. 1*B* and 2*A*). This discrepancy raised the possibility that CPS1 may be normally secreted luminally into bile in the polarized hepatocytes in vivo. To test this hypothesis, we collected bile from the common bile duct (CBD) of mice at 20-min intervals. Interestingly, the collected bile showed surprisingly high levels of CPS1, while no CPS1 was detected in serum (Fig. 2*B*). Transferrin and amylase were observed in mouse bile and serum as expected, consistent with the majority of bile proteins being derived from plasma (22). Similar findings were noted in human bile samples collected from the CBD, with some variability among individuals (*SI Appendix*, Fig. S4). Consistent with the CPS1 in serum or culture media of hepatocytes, bile CPS1, unlike transferrin and albumin, was observed in the 100,000 × *g* pellet fraction and the supernatant (Fig. 2*C*). CPS1 in the pelleted bile fraction was separated in the higher sucrose concentration fractions (Fig. 2*D*), but even CPS1 in the bile supernatant (Fig. 2*D*) sedimented in fractions similar to those seen in the supernatant fraction of mouse serum (*SI Appendix*, Fig. S2*A*). Ultrastructural analysis using immunogold staining of normal mouse liver showed CPS1 within and near liver canaliculi (Fig. 2*E*). Mass spectrometry of proteins from mouse bile, obtained from the gallbladder (GB) and CBD, identified 1,792 proteins (Fig. 2*F*, *SI Appendix*, Fig. S5, and Dataset S1). Notably, many mitochondrial proteins and all five enzyme components of the urea cycle—in addition to LDH, PDH, and the two exosome markers, CD9 and TSG101—were found in bile (Fig. 2*G*). CPS1 had a shorter half-life in bile than transferrin and albumin, and GB bile had detectable pancreatic enzymes (likely due to reflux from the pancreatic duct) (*SI Appendix*, Fig. S6), which explains the near-absent CPS1 level in GB bile (*SI Appendix*, Fig. S5*B*). Hence, our data suggest that CPS1 is normally released to bile canaliculus via the hepatocyte apical membrane, but is rerouted to the sinusoids upon hepatotoxicity, thereby rendering it readily detectable in serum during liver injury.

Uptake of Serum CPS1 by Macrophages. Next we investigated the mechanism of rapid serum CPS1 clearance in humans and mice during liver injury (12). To investigate whether CPS1 is degraded by serum proteases, serum from the FL-treated mice was incubated (37 °C) and tested over time. Serum CPS1 was not degraded after

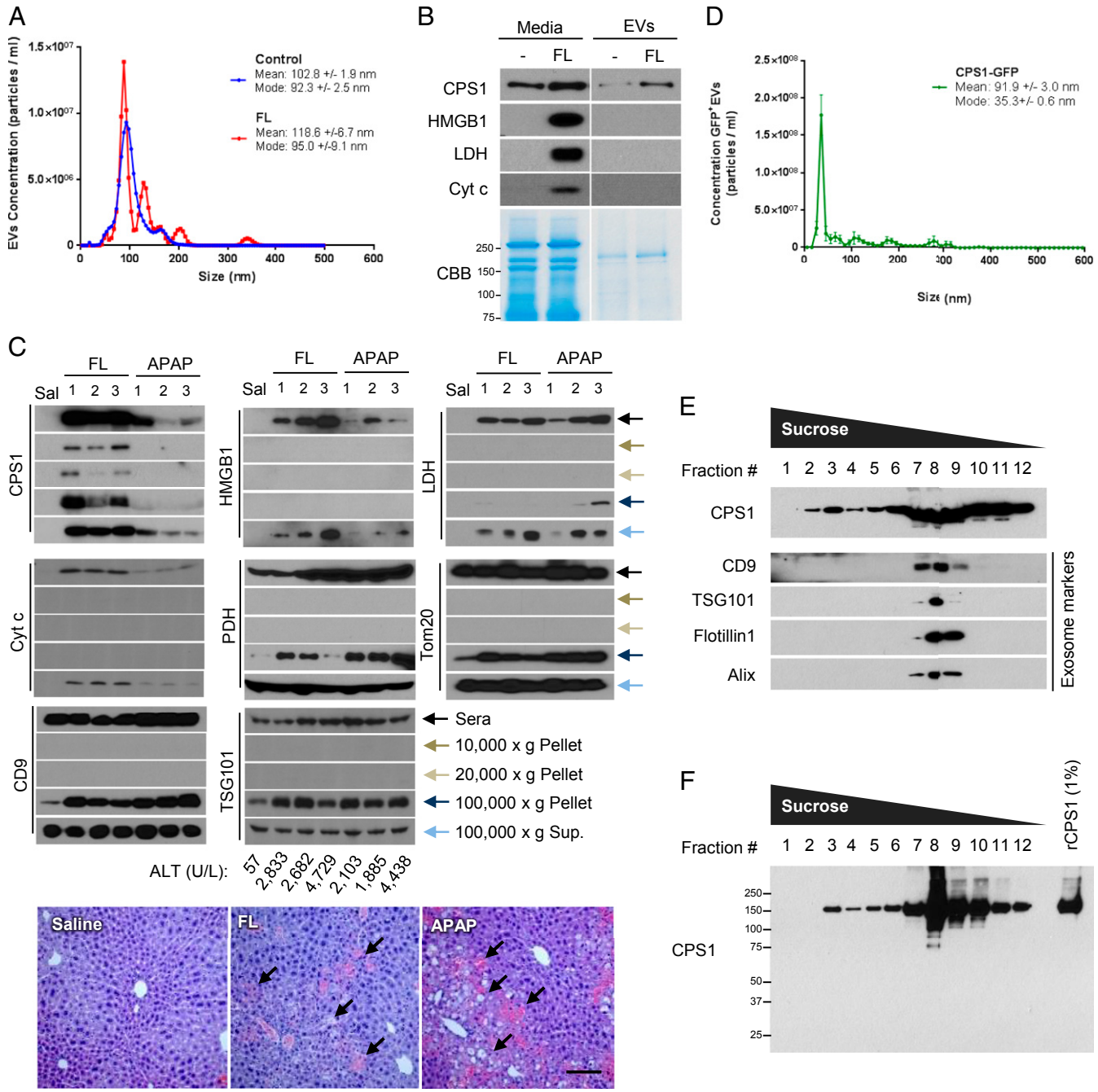

Fig. 1. CPS1 is released as a soluble multimeric protein that cosediments with EVs. (*A*) Size measurement of primary mouse hepatocyte-derived EVs by NTA. The numbers show mean and mode sizes ± SE. (*B*) Immunoblotting of culture media or EVs from primary hepatocytes preincubated with saline or FL (0.5 μg/mL, 4 h). Coomassie brilliant blue staining (CBB) is shown as a loading control. (*C*) Sera were collected from saline-injected mice (Sal) used as control, and from FL- or APAP-administered mice (three mice/group). Immunoblotting of intact mouse serum or pelleted serum components was carried out from the indicated sedimentation fractions. Blotting was done using antibodies to the indicated proteins. Serum ALT is included at the bottom of the *Middle* panels, in addition to a representative H&E staining of the liver (*Bottom*) (arrows highlight areas of injury). (Scale bar, 100 μm.) (*D*) NTA of GFP^+ particles isolated from primary hepatocytes that were transduced with lentiviral CPS1-GFP. The numbers show mean and mode sizes ± SE. (*E* and *F*) Sucrose gradient separation of the 100,000 × *g* pellet from culture media of primary hepatocytes (*E*) or of rCPS1 (*F*). In *F*, 1% of starting material (rCPS1) was loaded in the last lane as a reference control.

24 h, in contrast with HMGB1 (Fig. 3*A*), thereby indicating that serum proteases are not responsible for the rapid turnover of CPS1. We then examined whether serum CPS1 is taken up by endothelial cells or leukocytes. Primary endothelial cells from mouse aorta or human Jurkat T cells did not take up CPS1 (Fig. 3 *B* and *C*), while Mϕ from peripheral blood mononuclear cells (PBMC-Mϕ) of mice injected with FL accumulated CPS1 (Fig. 3*D*). Similarly, CPS1 was specifically taken up by the J774 Mϕ cell line incubated with hepatocyte culture media containing CPS1 (Fig. 3*E*). To further examine whether CPS1 is taken up by Mϕ, we generated His-tagged full-length human rCPS1 and a human transferrin (rTF) variant (a mutant form unable to bind iron) as a control (*SI Appendix*, Fig. S3*A*). Intravenous administration of rCPS1 into naïve mice showed a fast in vivo turnover

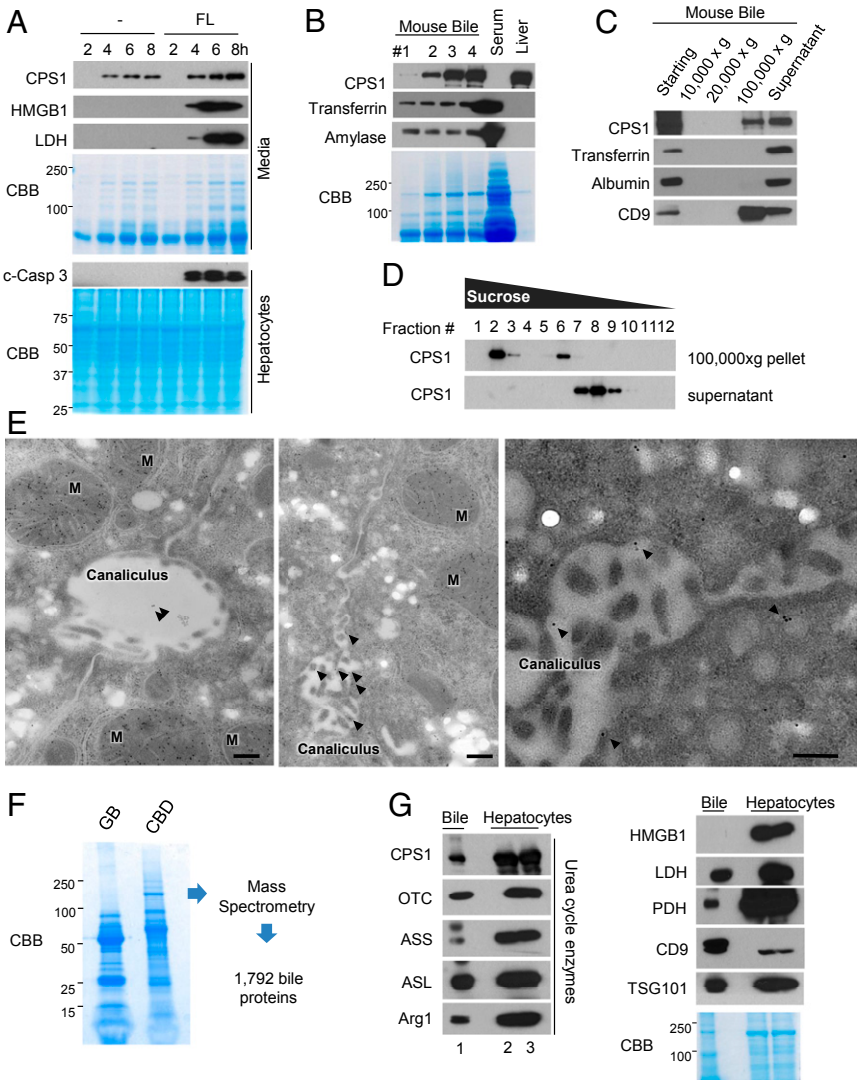

Fig. 2. CPS1 is secreted through bile canaliculi. (*A*) Mouse hepatocytes were treated with saline (-) or FL (0.5 μg/mL) for the indicated times. Abundance of CPS1, HMGB1, and LDH in the culture media, and of cleaved caspase 3 (c-Casp 3) in the cell lysates are shown. CBB are included to show equal protein loading. (*B*) Immunoblotting of mouse bile, serum, and liver lysates using antibodies to the indicated antigens. The bile was collected at 20-min intervals (#1–4 fractions). Similar results were observed from bile collections obtained from five other mice. (*C*) Mouse bile was pelleted using the indicated *g* forces, followed by analysis of the pelleted and supernatant fractions by immunoblotting. (*D*) Bile was pelleted at 100,000 × *g*, then the pellet and the supernatant fractions were analyzed by sucrose gradient sedimentation and immunoblotting similar to what was carried out in Fig. 1 *E* and *F*. (*E*) Mouse liver was prepared for transmission electron microscopy imaging. Immunogold staining of the liver sections was carried out using rabbit anti-CPS1 antibody followed by goat anti-rabbit antibody conjugated with 10-nm gold particles. Arrowheads highlight CPS1 within the bile canaliculus. (Scale bars, 200 nm.) M, mitochondria. A negative control that did not include the anti-CPS1 antibody did not manifest a significant gold particle signal. (*F*) Mouse bile was obtained from the GB or CBD then immediately analyzed by SDS/PAGE followed by staining using CBB. Each lane of the gel was analyzed by mass spectrometry (*SI Appendix*, Fig. S5). (*G*) Abundance of urea cycle enzymes and other proteins were analyzed by immunoblotting using bile (pooled collection from CBD, lane 1) and total cell extracts from primary hepatocytes (two independent isolations, lanes 2 and 3). All of the analyzed proteins were detected by mass spectrometry (as described in *F* and *SI Appendix*, Fig. S5).

rate ($T_{1/2}$ = 58 min) (Fig. 3*F*), consistent with the observation of rapid endogenous CPS1 turnover in blood during acute liver injury (12) and rat CPS1 half-life of 67 min in blood (17). Immunofluorescence analysis showed rCPS1 uptake by J774 Mϕ and human PBMC-Mϕ (Fig. 3 *G* and *H*), which supports the rapid clearance of CPS1 in vivo.

CPS1 Induces M2 Polarization of Monocytes and Hepatic Macrophages, Independent of Its Enzyme Activity. Hepatic Mϕs are comprised of liver-resident Kupffer cells, or bone marrow-derived monocytes recruited during liver disease conditions, and these cells actively participate in liver homeostasis (23). Given CPS1 uptake by monocytes/Mϕ, we examined if CPS1 activates Mϕ via the classic (M1) or alternative (M2) modes (24). While expression of M1-related (*CD64*/*CXCL10*/*IL6*) or M2-related (*MRC1*/*CCL22*/*IL10*) genes were elevated after incubation with LPS or IL-4, respectively (*SI Appendix*, Fig. S7), rCPS1 but not rTF significantly increased M2 gene expression (Fig. 4*A*). In contrast, *Arg1* expression was not altered by rCPS1 treatment of naïve Kupffer cells ex vivo (*SI Appendix*, Fig. S8*A*). However, rCPS1 administration significantly increased M2 gene expression (*Arg1*/*Mrc1*/*Il10*) of hepatic Mϕ (Fig. 4*B*) in association with Stat6 phosphorylation (*SI Appendix*, Fig. S8*B*). Moreover, transwell coculture of isolated naïve Kupffer cells with PBMCs from mice administered rCPS1 showed that factors released by the PBMCs induce M2 polarization of Kupffer cells without needing direct

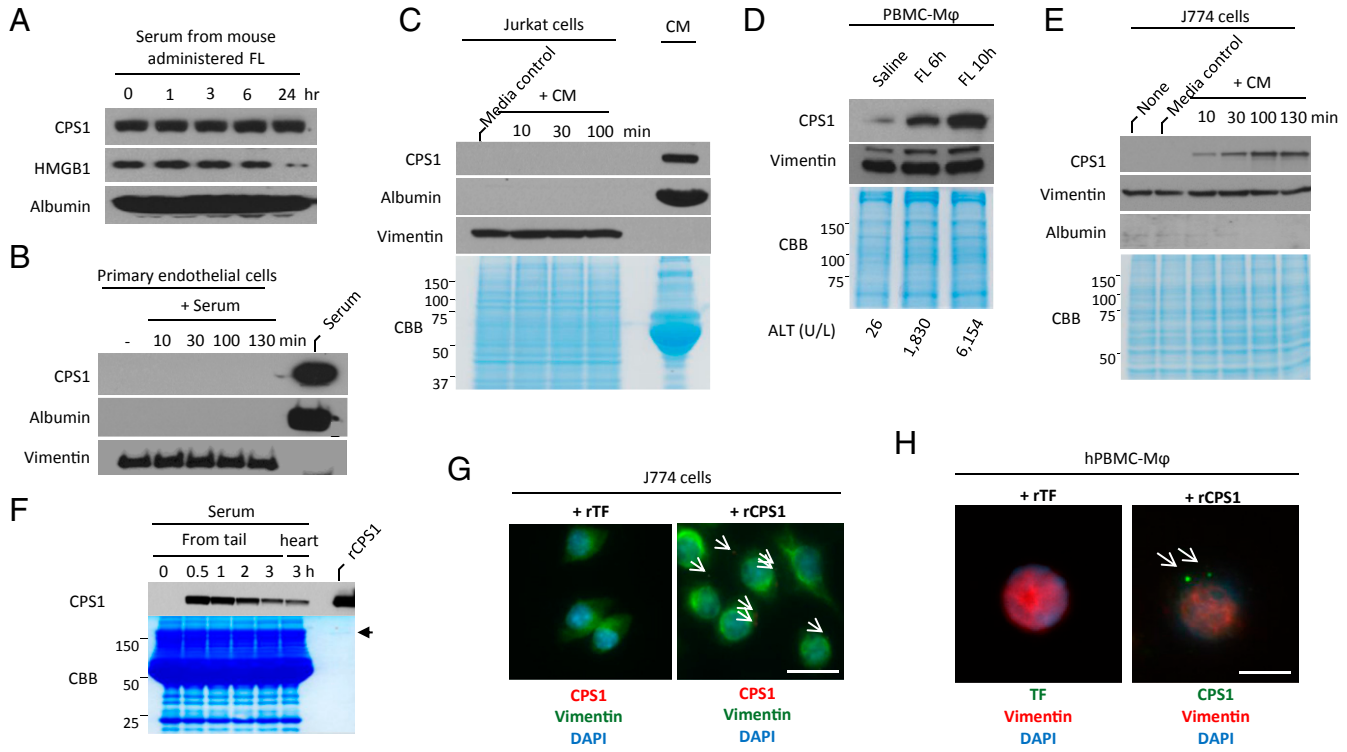

Fig. 3. CPS1 is taken up by mouse and human macrophages. (*A*) Serum from mice treated with FL was incubated at 37 °C for indicated time points, followed by immunoblotting using antibodies to the indicated proteins. (*B*) Primary endothelial cells were incubated with serum from a mouse pretreated with FL (0.15 mg/kg, 4 h). Immunoblot analysis of the cell lysates and the input serum was then carried out using antibodies to CPS1, albumin (as control serum protein), and vimentin (as control endothelial cell protein). (*C*) Jurkat cells were incubated with control media or conditioned media (CM) obtained from primary hepatocytes incubated with FL (0.5 μg/mL, 4 h). Immunoblot analysis of the Jurkat cell lysates and the input CM was then performed using antibodies to CPS1, albumin, and vimentin. CBB of a duplicate gel is included to profile the loaded proteins. (*D*) PBMCs from mice administered saline or FL were collected at 6 or 10 h postinjection. PBMC-Mϕ were analyzed by immunoblotting. Serum ALT levels are shown at the bottom. (*E*) J774 cells were cultured in their standard media (none), media for hepatocyte culture (media control), or CM from hepatocytes incubated with FL. Intracellular uptake of albumin (none detected) and CPS1 are shown. (*F*) Mice were administered rCPS1 followed by collection of 20 μL of blood at the indicated time point from tail (or heart at end of the experiment). The collected sera (2 μL) were then blotted with anti-CPS1 antibody and examined by CBB to ensure equal loading. (*G*) J774 cells were incubated with rTF (0.5 μg/mL) or rCPS1 (1 μg/mL). Immunofluorescence staining was done using antibodies to CPS1 and vimentin, followed by DAPI staining (nuclear). Arrows highlight CPS1 uptake in the cells. (Scale bar, 20 μm.) (*H*) Immunofluorescence staining of human PBMC-Mϕ pretreated with rTF or rCPS1, using antibodies to TF/vimentin and CPS1/vimentin followed by staining with DAPI. Arrows highlight rCPS1 uptake. (Scale bar, 10 μm.)

contact (Fig. 4*C*). Notably, *Cxcr2* and *Ccr1* expression was the most reduced among the chemokine signaling pathway genes in hepatic Mϕ from the rCPS1-APAP–administered mice as compare with the rTF-APAP–administered mice (*SI Appendix*, Fig. S9*A*). In line with the inflammatory roles of CXCR2 and CCR1 (25–27), their gene expression was decreased by IL-4 treatment and their down-regulation by rCPS1 was validated by independent qPCR of hepatic Mϕ from mice injected with rCPS1 or rTF (*SI Appendix*, Fig.S9 *B* and *C*). These results suggest that CPS1 in serum elicits an antiinflammatory role via Mϕ during liver injury.

Given the heterogeneity of hepatic Mϕ, we examined if CPS1 could promote recruitment of circulating monocytes to the liver. PBMC-Mϕ, bone marrow cells, and hepatic Mϕ, isolated from the same mice 12 or 24 h postadministration of recombinant proteins, showed that *Arg1* expression in PBMC-Mϕ and bone marrow cells peaked much earlier (at 12 h), while hepatic Mϕ activation followed at 24 h (Fig. 4*D*). Homing to the liver was validated by isolating PBMC-Mϕ from mice injected with rTF or rCPS1, labeling with PKH26, then reinjecting into mice followed by isolation of the hepatic Mϕs to test for the presence of labeled cells (*SI Appendix*, Fig. S10). Notably, 16% of the terminally isolated F4/80$^+$ hepatic Mϕs harbored PKH26 dye (i.e., representing PBMC-Mϕ from mice preactivated with rCPS1 that homed to the liver), while only 1% of the cells preactivated with rTF costained with PKH26 (Fig. 4*E*). Hence, CPS1 elicits PBMC-Mϕ M2-polarization in blood or bone marrow, with subsequent homing of these activated cells to the liver. Importantly, the rCPS1 T471N mutant (*SI Appendix*, Fig.S3 *C* and *D*), which is enzymatically inactive (16), did not alter the effect of CPS1 on M2 gene expression (Fig. 4*F*), thereby indicating that the cytokine-like role of CPS1 is independent of its enzymatic activity.

Prophylactic and Therapeutic Effects of rCPS1 in Experimental Liver Injury. Contrary to the proinflammatory M1 Mϕs, the antiinflammatory M2 Mϕs are involved in repair and proliferation (24). Thus, we examined if CPS1 has a protective role during liver injury. Mice were given rTF or rCPS1, then injected with saline or FL after 24 h. rTF-FL–administered mice had elevated alanine transaminase (ALT), cell death, and liver hemorrhage as expected, whereas rCPS1-FL–administered mice had limited ALT elevation and significantly less histologic liver damage (Fig. 5 *A* and *B*). Release of CPS1/HMGB1/LDH were greatly attenuated in rCPS1-FL mice, compared with rTF-FL mice, along with decreased apoptosis in the livers (determined by cleaved caspase-3 and -7 and TUNEL staining) (Fig. 5 *C*–*E*). The F4/80$^+$ Mϕ number increased significantly in livers of mice given rCPS1, while Ki-67$^+$ cells increased but did not reach statistical significance (Fig. 5 *F* and *G*). In addition, rCPS1 led to >threefold increase in phagocytic activity of hepatic Mϕs (Fig. 5*H*), which may contribute to debris clearance. Hence, rCPS1 leads hepatic

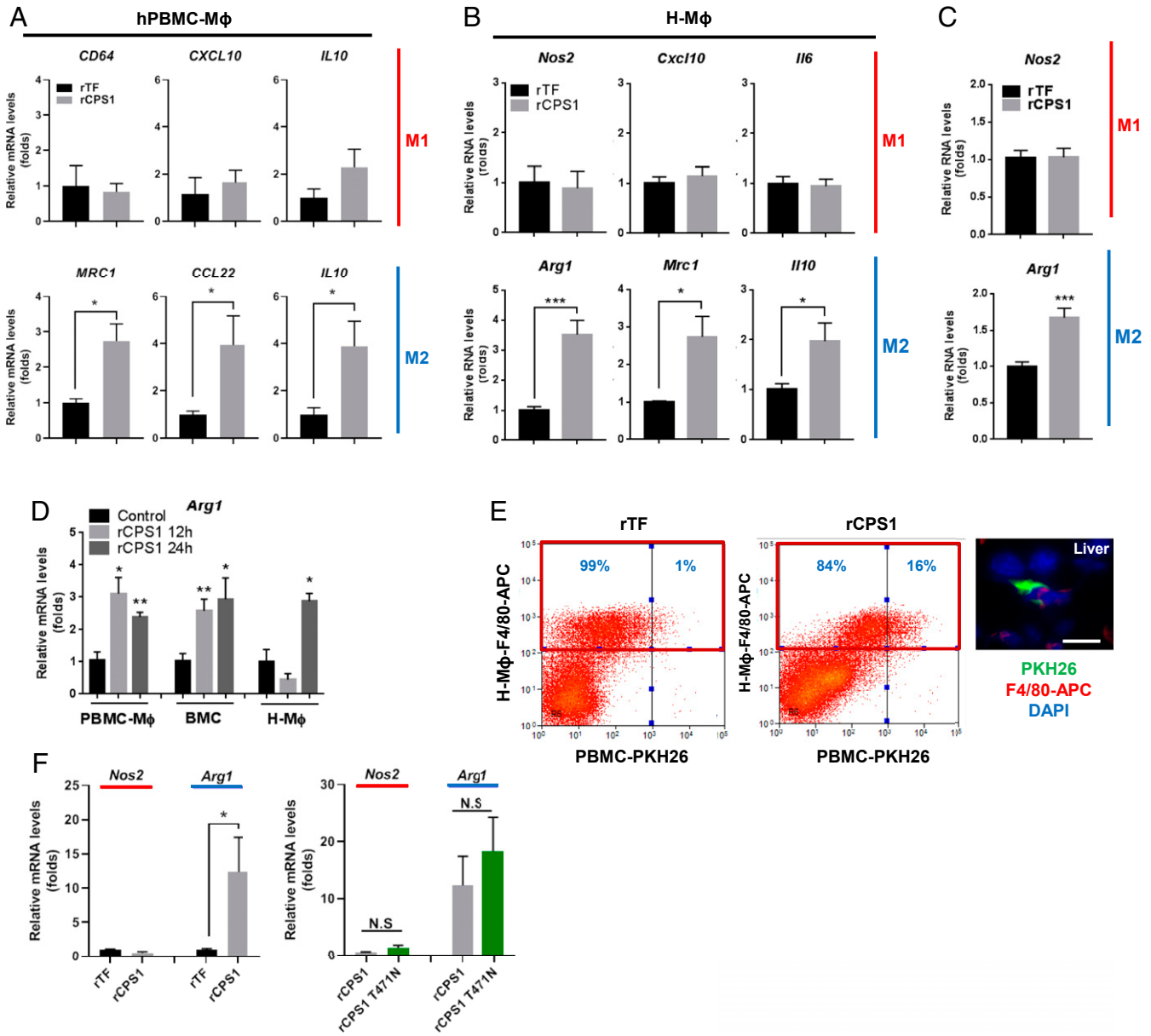

Fig. 4. CPS1 induces M2 polarization of macrophages. (*A*) Human Mϕ from PBMCs (hPBMC-Mϕ, $n = 5$ per group) were treated with rTF (0.5 μg/mL) or rCPS1 (1 μg/mL) for 24 h, followed by qPCR analysis of the indicated transcripts. (*B*) Hepatic Mϕ (H-Mϕ) were isolated from mice injected with rTF (25 μg, $n = 7$) or rCPS1 (50 μg, $n = 8$) 24 h before the cell isolation, followed by qPCR analysis. (*C*) PBMCs were isolated from mice injected with rTF (25 μg) or rCPS1 (50 μg), then cocultured in transwell plates (*Upper*) with naïve Kupffer cells isolated from other mice (*Lower*) ($n = 6$ per group). After 24 h coculture, *Nos2* and *Arg1* expression in the Kupffer cells was analyzed by qPCR. (*D*) Mice were injected with rTF (control, 24 h) or rCPS1 12 or 24 h before killing ($n = 3$ per group). PBMC-Mϕ, bone marrow cells (BMC), and H-Mϕ were isolated from the mice and *Arg1* mRNA was analyzed by qPCR. (*E*) PBMCs were isolated from mice injected with rTF or rCPS1, labeled with PKH26, then injected to another naive mouse. The H-Mϕ were isolated and stained with APC-labeled F4/80 antibody for flow cytometry analysis. The ratio of F4/80$^+$ to PKH26$^-$ versus F4/80$^+$ to PKH26$^+$ cells (%) are included (red boxes). (*Right*) Immunofluorescence image of F4/80$^+$ (green)/PKH26$^+$ (red) cells in the liver costained with DAPI (blue). (Scale bar, 10 μm.) Similar results were obtained in two other independent experiments. (*F*) J774 cells were treated with rTF (0.5 μg/mL), rCPS1 (1 μg/mL), or rCPS1 T471N (1 μg/mL, $n = 6$ per group) for 24 h followed by qPCR analysis of *Nos2* and *Arg1* expression. $^*P < 0.05$; $^{**}P < 0.01$; $^{***}P < 0.001$. N.S., not significant.

Mϕs to proliferate and undergo M2 polarization to an antiinflammatory phenotype. The CPS1 protective effect is likely mediated by Mϕ cytokines, because hepatic Mϕ-conditioned media isolated from rCPS1-injected—but not rTF-injected—mice decreased hepatocyte cell death and elevated Ki-67 and phosphorylated-Rb upon FL treatment (*SI Appendix*, Fig. S11).

We also tested the effect of CPS1 on APAP-induced liver injury, which more closely mimics human drug-induced liver injury. Administration of rCPS1 24 h before exposure to APAP attenuated liver damage significantly as determined by serum ALT, liver histology, and serum levels of CPS1/HMGB1/LDH (Fig. 6 *A*–*C*). TUNEL$^+$ cells were decreased while F4/80$^+$ Mϕ and to Ki-67$^+$ cells increased upon APAP exposure in the rCPS1 versus the control rTF group (Fig. 6 *D*–*F*). Notably, rTF alone does not impact the extent of FL- or APAP-induced liver injury (*SI Appendix*, Fig. S12), thereby indicating that the protective effect imparted by rCPS1 is not related to a damaging effect that is mediated by rTF. We also tested the importance of

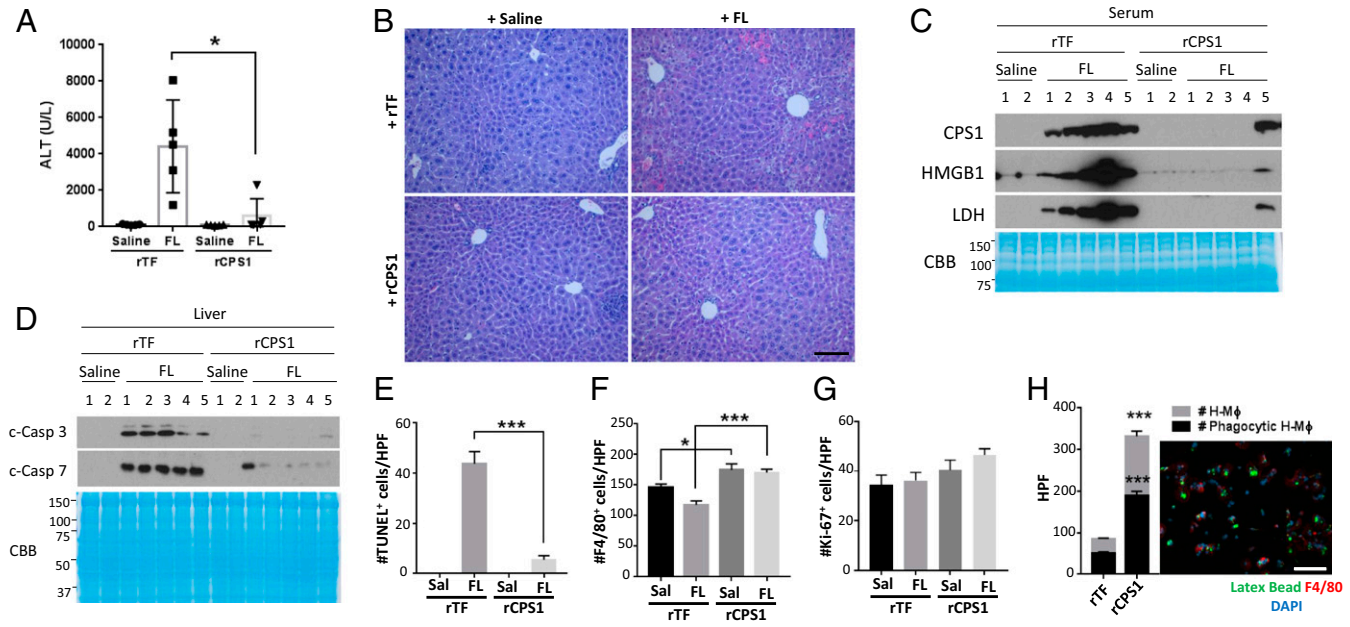

Fig. 5. FL-induced liver injury is attenuated by preinjection of recombinant CPS1. (*A*) Mice were injected with rTF (25 μg) or rCPS1 (50 μg, 10 mice per group). After 24 h, each group was subdivided such that five mice were injected with saline and five mice were injected with FL (0.15 mg/kg). Serum ALT was then measured (*$P < 0.05$). (*B*) Representative H&E staining of livers from the mice used in *A*. (Scale bar, 200 μm.) (*C* and *D*) Immunoblot analysis of serum proteins (*C*) and liver lysates (*D*) from the four subgroups in *A*. The tested antigens are as indicated, together with CBB stainings as loading controls. c-Casp 3, cleaved caspase 3; c-Casp 7, cleaved caspase 7. (*E*–*G*) Livers from mice used in *A* were subjected to TUNEL or immunofluorescence staining using antibodies to F4/80 or to Ki-67. Positive cells were counted from five randomly acquired images (HPF, high-power field). *$P < 0.05$, ***$P < 0.001$. (*H*) Hepatic Mϕ (H-Mϕ) were isolated from mice injected with rTF ($n = 3$) or rCPS1 ($n = 3$) followed by testing their phagocytosis capacity via uptake of FITC-labeled IgG-coated latex beads. F4/80-labeled (red, total H-Mϕ) or FITC-labeled (green, phagocytic H-Mϕ) were counted. (Scale bar, 50 μm.) ***$P < 0.001$. Note the marked increase in numbers of H-Mϕ and phagocytic H-Mϕ after rCPS1 administration to the mice.

macrophages in the observed CPS1 protective effect. For this, macrophages were depleted using clodronate liposome administration (Fig. 6*G*), and this depletion blocked the protective effect of CPS1 as determined by serum ALT and TUNEL staining analysis (Fig. 6 *H* and *I*). This provides supportive evidence that CPS1 attenuation of liver injury occurs through Mϕs.

More relevant to potential human application, the administration of rCPS1 3 h post-APAP exposure, when serum ALT levels are highly elevated (average ALT > 2,000), also led to more rapid recovery from liver injury compared with rTF-injected mice (Fig. 6*J*). Consistent with this, serum HMGB1 and LDH were markedly lower in sera of APAP-rCPS1 mice compared with APAP-rTF mice (Fig. 6*K*). These overall findings indicate that CPS1 serves as a hitherto unappreciated antiinflammatory cytokine that may provide potential therapeutic benefit in the setting of acute liver injury (Fig. 7).

Discussion

CPS1 was previously identified as a readily detected protein released from apoptotic hepatocytes (12). Serum CPS1 was suggested as a biomarker for the resolution of acute liver injury given its tissue-specific expression, abundance, and rapid turnover in serum ($T_{1/2} \sim 2$ h) compared with the commonly utilized ALT (12, 17). These earlier observations led us to probe the mechanism of CPS1 release and its short half-life in blood. We find that CPS1 is nonclassically secreted, and its release occurs regardless of liver damage but through different routes, depending on the presence or absence of liver damage. Biliary release of CPS1 is an unexpected finding along with the identification of several other mitochondrial proteins in bile. The rapid clearance of serum CPS1 occurs via uptake by circulating monocytes, which in turn elicits their activation into antiinflammatory cells that home to the liver and protect from liver injury induced by FL or APAP. The cytokine-like antiinflammatory promoting effect of CPS1 is enzyme-independent and involves PBMC-Mϕ and bone marrow cells, although immune cells in other tissue compartments may be potential targets. These findings suggest that CPS1 may serve as a therapeutic in acute liver injury.

Most cells, including hepatocytes, release context-dependent EVs. CPS1 was previously reported as a component of cultured rat hepatocyte-derived exosomes based on proteomic findings (19). However, our data indicate that CPS1 that is collected using standard exosome preparation methods primarily partitions with the exosome fraction because of its propensity to oligomerize and form multimers rather than being a component of EVs. This is based on biochemical assessment after sucrose gradient sedimentation of rCPS1 or CPS1 found in blood or bile, or upon ultrastructural evaluation. We posit that the aggregation propensity of CPS1 could increase its accessibility, recognition, and uptake by pino-/phago-cytosis of Mϕ (28), although the precise mechanism of its uptake and the smallest domain of CPS1 that imparts its antiinflammatory function remain to be defined.

Presence of CPS1 in Bile. Biliary secretion of CPS1 was an unexpected finding. While nonprotein bile components are well characterized, only a limited number of bile proteins have been identified due to technical challenges (29). Proteomic analysis has identified several proteins in bile (30–40). Notably, CPS1 has not been reported previously as a human bile component, although another urea cycle enzyme, ornithine transcarbamylase, was reported nearly 60 y ago as a bile component, and was studied as a potential marker of liver disease (41–45). Our findings herein show that CPS1 is found in both mouse and human bile but the detection of CPS1 by immunoblotting of human bile was feasible only upon using fresh bile together with acetone precipitation of the protein fraction, while detection of

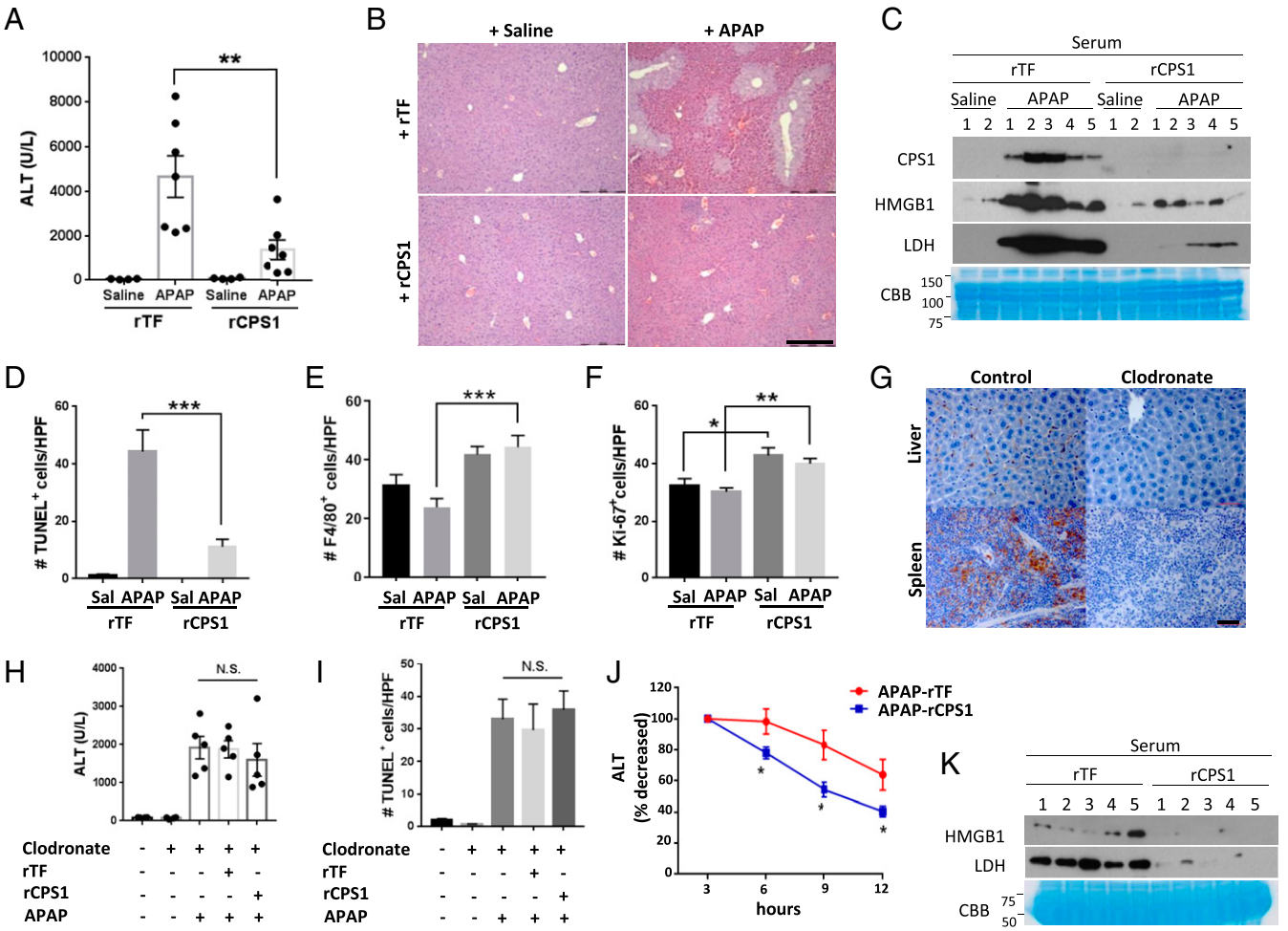

Fig. 6. APAP-induced liver injury is attenuated by administration of rCPS1 prophylactically and therapeutically through Mϕs. (*A–C*) Male mice were injected via tail vein with rTF (25 μg) or rCPS1 (50 μg) 24 h before intraperitoneal APAP (350 mg/kg mouse weight) or saline administration. After 4 h, the mice [rTF-saline (n = 4), rTF-APAP (n = 7), rCPS1-saline (n = 4), rCPS1-APAP (n = 7)] were killed followed by analysis of the serum ALT (*A*, $^{**}P < 0.01$) and liver tissue histology using H&E staining (*B*). (Scale bar, 200 μm.) Immunoblot analysis of the sera using antibodies to the indicated antigens is shown (*C*, CBB is included as a loading control). (*D–F*) Livers from *A–C* were subjected to TUNEL or immunofluorescence staining using antibodies to F4/80 or Ki-67. Quantification was carried out by counting positive-staining cells in a blinded fashion from five randomly selected images from each liver (HPF, high-power field). $^{*}P < 0.05$, $^{**}P < 0.01$, $^{***}P < 0.001$. (*G–I*) Mice were administered clodronate liposomes or PBS 48 h before injection of rTF or rCPS1. After another 24 h, the mice were given APAP or saline [control (n = 4), clodronate (n = 4), clodronate-APAP (n = 5), clodronate-rTF-APAP (n = 5), clodronate-rCPS1-APAP (n = 5)]. F4/80 staining of liver and spleen showed Mϕ depletion in liver and spleen of clodronate-treated mice (*G*). (Scale bar, 50 μm.) Serum ALT levels and TUNEL staining of the livers are also shown (*H* and *I*). N.S., no significance between any two of groups 3–5. Note that the ALT values in *H* (clodronate+APAP) are lower than those in *A* (APAP+rTF) but the experiments were carried out independently and do not imply that clodronate alone protects from APAP-induced injury [others have shown that clodronate may exacerbate APAP-induced liver injury (27)]. (*J* and *K*) Mice (n = 30) were administered APAP intraperitoneally, followed 3 h later by tail vein injection with rTF or rCPS1 (15 mice per group). Serum was collected from the tail veins of the mice at 3-h intervals. *J* shows the serum ALT levels, presented as percentage decrease compared with the values at the 3 h time point after APAP administration. $^{*}P < 0.05$. *K* shows the immunoblot analysis of serum from five representative mice per group.

CPS1 in mouse bile did not require acetone precipitation. Notably, even short-term storage of human bile at −80 °C leads to degradation and loss of CPS1 detection.

The function of CPS1 and other mitochondrial proteins in bile remains to be determined, but the stoichiometry of CPS1 that is released into bile compared with total liver CPS1 is very small. We estimate that 0.002% of mouse liver CPS1 is excreted into bile per hour (based on sequential collection of bile followed by immunoblotting). Although the relative bile content of CPS1 is very small compared with hepatocytes, the absolute amount may not be trivial given the abundance of CPS1. Notably, the amount of CPS1 released to culture media of healthy primary mouse hepatocytes is comparable to the amount released by dying cells when other damage marker proteins also become readily detectable (Figs. 1*B* and 2*A* and *SI Appendix*, Fig. S1). Therefore, the presence of CPS1 and the other urea cycle enzymes in bile, which is mimicked by the constitutive release of CPS1 by cultured hepatocytes, is unlikely to be part of simple enzyme turnover but is potentially related to a novel release pathway by hepatocytes that remains to be defined. If one considers an endosymbiotic origin of mitochondria from prokaryotes (46), release of mitochondrial proteins may be an aspect of protein secretion of ancestral bacteria. Of note, ammonia (47) and urea (48) have been measured in bile, which raises the possibility that bile could also remove ammonia via CPS1 aside from the liver.

An Immune Function for CPS1. The liver serves an immune function through hepatocyte secretion of specific proteins into blood (49), and harbors the largest number of Mϕ (~80% of body's total) (23). Proteins released from hepatocytes into sinusoids could

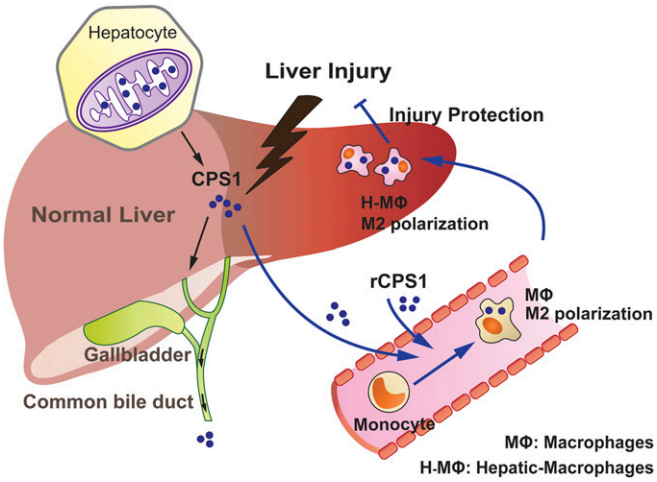

Fig. 7. Schematic model of CPS1 release and the biologic function of released CPS1. In normal liver, hepatic mitochondrial CPS1 is continuously secreted to bile (black arrows) while being undetectable in blood. Upon acute liver injury, CPS1 is released to the bloodstream where it is rapidly taken up by circulating monocytes and leads to their M2 polarization and homing to the liver independent of CPS1 enzyme activity (blue arrows). The endogenous CPS1-induced antiinflammatory properties of M2-Mϕ protection from liver injury can also be provided therapeutically upon administration of recombinant CPS1 in experimental APAP-induced liver injury.

interact and communicate with liver-resident Kupffer cells and circulating monocytes. Kupffer cell activation and recruitment of circulating monocytes have been demonstrated in mice administered with APAP (50–54). In addition, the presence of human Mϕ within an antiinflammatory/regenerative microenvironment of the liver was observed in patients with APAP-induced acute liver failure, suggesting a beneficial effect of hepatic Mϕ (50). In line with these observations, circulating CPS1 protected from APAP- or FL-induced liver damage, at least partially, via triggering M2 polarization of bone marrow-derived monocytes and hepatic Mϕ in a CPS1 enzyme-independent manner. In addition to IL-4 and IL-13 that induce M2 polarization through IL-4R, our findings highlight CPS1 as another potential M2 inducer. Considering that 10–50 ng/mL of IL-4 is generally used to induce M2 polarization ex vivo, the stoichiometry of rCPS1 we used (1 μg/mL) is comparable to IL-4 (after correcting for the much smaller IL-4 protein size), albeit the precise mechanism underlying Mϕ activation by CPS1 remains to be elucidated. Like HMGB1, which triggers the release of proinflammatory cytokines via TLR4 or RAGE binding (7), CPS1 may be recognized by a specific receptor on Mϕ and may signal through phagocytosis-dependent or -independent modes. Taken together, our findings (Fig. 7) show that the mitochondrial protein CPS1 is normally released into bile, and demonstrate a direct antiinflammatory M2 polarization effect of CPS1 that is independent of its enzyme activity. The ability of rCPS1 that is administered intravenously after injury to ameliorate APAP-induced liver injury raises the exciting possibility of its utility as a therapeutic in select cases of acute liver injury.

Materials and Methods

Mouse Experiments, Primary Cell Isolation, and Culture. Mouse procedures were approved by the University Committee on Use and Care of Animals at the University of Michigan. We isolated and cultured hepatocytes, Mϕs from PBMCs, hepatic Mϕs, aortic endothelial cells, and bone marrow cells from mice. Detailed information is provided in *SI Appendix, SI Materials and Methods*.

Microarray Analysis. Total RNA of hepatic Mϕ from mice, injected with rCPS1 or rTF ($n = 4$ per group) followed by APAP administration, was converted to cDNA and biotinylated as recommended by Affymetrix GeneChip WT PLUS. See *SI Appendix, SI Materials and Methods* for more details.

Flow Cytometry. For experiments testing circulating monocyte homing to the liver, 8-wk-old male FVB/N mice were administered rTF or rCPS1 as described above. After 12 h, PBMCs were isolated, stained with PKH26 (Sigma) for 2 min, followed by washing 4× as per the manufacturer's recommendation, then injected into mice via tail vein (2×10^5 cells in 150 μL of PBS). At 24 h postinjection, hepatic Mϕ were isolated and incubated with APC-labeled F4/80 antibodies (20 min, on ice, in dark) followed by washing 3× (300 × *g*, 5 min). Single color controls were included for gating purposes. The cells were analyzed on a Beckman Coulter MoFlo Astrios at the University of Michigan Flow Cytometry Core Facility.

Isolation of EVs, Sucrose Gradient Separation, and Biochemical Analysis. EV isolation and sucrose gradient separation were carried out as described previously (55) with slight modifications. See *SI Appendix, SI Materials and Methods* for details.

Quantitative RT-PCR. RNA was extracted in TRIzol (Invitrogen) and isolated according to the manufacturer's protocol, then 1 μg of RNA was reverse transcribed to cDNA using TaqMan reverse-transcriptase kit (Applied Biosystems). qPCR was done using Brilliant SYBR Green Master Mix (Bio-Rad) and Eppendorf MasterCycler RealPlex (Thermo Fisher Scientific). Primer information is included in *SI Appendix*, Table S2.

Bile Collection. Mice were anesthetized with isoflurane and a PE-08 catheter was inserted into the CBD using a dissecting microscope and glued in place. The mice were maintained under anesthesia and placed under a warming lamp, and bile was collected at 20-min intervals for 2 h in microcentrifuge tubes containing Protease Inhibitor Mixture (Invitrogen).

For human bile studies, bile was collected from patients undergoing endoscopic retrograde cholangiopancreatography for indicated clinical reasons (carried out at the University of Michigan Medical Center under an institutional review board-approved protocol) (*SI Appendix*, Fig. S4*B*). For immunoblotting, 1 mL of human bile was precipitated with six volumes of −20 °C acetone (overnight, −80 °C) to remove interfering substances, followed by centrifugation. The pellet was dissolved in 200 μL of Tris-glycine SDS-containing sample buffer, and 10 μL from each sample was subjected to SDS/PAGE followed by immune blotting.

Protein Identification by LC/MS-MS. Mouse bile samples collected from the CBD or the GB were analyzed by mass spectrometry. See *SI Appendix, SI Materials and Methods* for details.

Nanoparticle Tracking Analysis. For measuring particle size and concentration, samples were diluted with PBS to be in a range between 20 and 80 particles per frame, then analyzed using scatter mode of the NanoSight NS300 instrument (at 23.3 °C; syringe pump at 20 μL/min). Five videos of 1 min each documenting Brownian motion of nanoparticles were recorded, followed by analysis using NanoSight software. To analyze the GFP-containing particles, samples were analyzed under the fluorescence mode with a 488-nm wavelength laser.

Immunofluorescence Staining and Immunogold-Staining Electron Microscopy. Five-micrometer-thick paraffin sections of liver were deparaffinized with xylene and rehydrated through a series of graded ethanol. Detailed information is provided in *SI Appendix, SI Materials and Methods*.

Expression and Purification of Recombinant Proteins. Insect cell expression and purification of human CPS1 were performed as described previously (56) with slight modification. Briefly, pFastBac-hCPS1 or pFastBac-hTF mutant with His-tag was generated, then, recombinant proteins were expressed using a baculovirus system. See *SI Appendix, SI Materials and Methods* for details.

CPS1 Activity. CPS1 enzymatic activity was measured using the hydroxyurea method as described previously (57). See *SI Appendix, SI Materials and Methods* for details.

TUNEL Assay. Cell death was detected using an ApopTag Red In Situ Apoptosis detection Kit (EMD Millipore). Briefly, deparaffinized liver sections were incubated in a humidified chamber (37 °C, 1 h) with TdT enzyme solution, and applied to antidigoxigenin conjugate solution (rhodamine) for 30 min

(22 °C) in the dark. After washing, the slides were mounted and images were acquired.

Phagocytosis Assay. Phagocytic activity was detected using a Phagocytosis assay kit (Cayman) according to the manufacturer's protocol. See *SI Appendix, SI Materials and Methods* for details.

Statistics. Data are presented as mean ± SEM and graphed using GraphPad Prism 7. Data are representative of two to four independent experiments. The statistical significance was assessed using an unpaired two-tailed Student's *t* test for single comparisons or a one-way ANOVA with post hoc Tukey's test for multiple group comparisons. $P < 0.05$ was considered to be statistically significant and was compared as $*P < 0.05$, $**P < 0.01$, $***P < 0.001$.

ACKNOWLEDGMENTS. We thank Bradley Nelson and Yang Song for excellent technical support in the electron microscopy experiments and figure preparation, respectively. This work was supported by the National Institutes of Health Grant R01 DK47918 (to M.B.O.); Postdoctoral Clinical and Translational Science Award from National Institutes of Health Grant UL1TR002240 (to M.-J.P.); and National Institutes of Health Grant P30 DK34933 to the University of Michigan.

1. Bernal W, Wendon J (2013) Acute liver failure. *N Engl J Med* 369:2525–2534.
2. Lee WM (2013) Drug-induced acute liver failure. *Clin Liver Dis* 17:575–586, viii.
3. Antoine DJ, et al. (2012) Molecular forms of HMGB1 and keratin-18 as mechanistic biomarkers for mode of cell death and prognosis during clinical acetaminophen hepatotoxicity. *J Hepatol* 56:1070–1079.
4. Ilmakunnas M, et al. (2008) High mobility group box 1 protein as a marker of hepatocellular injury in human liver transplantation. *Liver Transpl* 14:1517–1525.
5. Kostova N, Zlateva S, Ugrinova I, Pasheva E (2010) The expression of HMGB1 protein and its receptor RAGE in human malignant tumors. *Mol Cell Biochem* 337:251–258.
6. Yan W, et al. (2012) High-mobility group box 1 activates caspase-1 and promotes hepatocellular carcinoma invasiveness and metastases. *Hepatology* 55:1863–1875.
7. Bianchi ME, et al. (2017) High-mobility group box 1 protein orchestrates responses to tissue damage via inflammation, innate and adaptive immunity, and tissue repair. *Immunol Rev* 280:74–82.
8. Eleftheriadis T, Pissas G, Liakopoulos V, Stefanidis I (2016) Cytochrome *c* as a potentially clinical useful marker of mitochondrial and cellular damage. *Front Immunol* 7: 279.
9. Miller TJ, et al. (2008) Cytochrome *c*: A non-invasive biomarker of drug-induced liver injury. *J Appl Toxicol* 28:815–828.
10. Chen GY, Nuñez G (2010) Sterile inflammation: Sensing and reacting to damage. *Nat Rev Immunol* 10:826–837.
11. Szabo G, Petrasek J (2015) Inflammasome activation and function in liver disease. *Nat Rev Gastroenterol Hepatol* 12:387–400.
12. Weerasinghe SV, Jang YJ, Fontana RJ, Omary MB (2014) Carbamoyl phosphate synthetase-1 is a rapid turnover biomarker in mouse and human acute liver injury. *Am J Physiol Gastrointest Liver Physiol* 307:G355–G364.
13. Clarke S (1976) A major polypeptide component of rat liver mitochondria: Carbamyl phosphate synthetase. *J Biol Chem* 251:950–961.
14. Nicoletti M, Guerri C, Grisolia S (1977) Turnover of carbamyl-phosphate synthase, of other mitochondrial enzymes and of rat tissues. Effect of diet and of thyroidectomy. *Eur J Biochem* 75:583–592.
15. de Cima S, et al. (2015) Structure of human carbamoyl phosphate synthetase: Deciphering the on/off switch of human ureagenesis. *Sci Rep* 5:16950.
16. Pekkala S, et al. (2010) Understanding carbamoyl-phosphate synthetase I (CPS1) deficiency by using expression studies and structure-based analysis. *Hum Mutat* 31: 801–808.
17. Ozaki M, et al. (1994–1995) Enzyme-linked immunosorbent assay of carbamoylphosphate synthetase I: Plasma enzyme in rat experimental hepatitis and its clearance. *Enzyme Protein* 48:213–221.
18. Kim J, et al. (2017) CPS1 maintains pyrimidine pools and DNA synthesis in KRAS/LKB1-mutant lung cancer cells. *Nature* 546:168–172.
19. Conde-Vancells J, et al. (2008) Characterization and comprehensive proteome profiling of exosomes secreted by hepatocytes. *J Proteome Res* 7:5157–5166.
20. Hirsova P, et al. (2016) Lipid-induced signaling causes release of inflammatory extracellular vesicles from hepatocytes. *Gastroenterology* 150:956–967.
21. Raposo G, Stoorvogel W (2013) Extracellular vesicles: Exosomes, microvesicles, and friends. *J Cell Biol* 200:373–383.
22. Mullock BM, et al. (1985) Sources of proteins in human bile. *Gut* 26:500–509.
23. Krenkel O, Tacke F (2017) Liver macrophages in tissue homeostasis and disease. *Nat Rev Immunol* 17:306–321.
24. Sica A, Invernizzi P, Mantovani A (2014) Macrophage plasticity and polarization in liver homeostasis and pathology. *Hepatology* 59:2034–2042.
25. Kuboki S, et al. (2008) Hepatocyte signaling through CXC chemokine receptor-2 is detrimental to liver recovery after ischemia/reperfusion in mice. *Hepatology* 48: 1213–1223.
26. Van Sweringen HL, et al. (2013) Roles of hepatocyte and myeloid CXC chemokine receptor-2 in liver recovery and regeneration after ischemia/reperfusion in mice. *Hepatology* 57:331–338.
27. Ju C, Tacke F (2016) Hepatic macrophages in homeostasis and liver diseases: From pathogenesis to novel therapeutic strategies. *Cell Mol Immunol* 13:316–327.
28. Pratten MK, Lloyd JB (1986) Pinocytosis and phagocytosis: The effect of size of a particulate substrate on its mode of capture by rat peritoneal macrophages cultured in vitro. *Biochim Biophys Acta* 881:307–313.
29. Farina A, Dumonceau JM, Lescuyer P (2009) Proteomic analysis of human bile and potential applications for cancer diagnosis. *Expert Rev Proteomics* 6:285–301.
30. Kristiansen TZ, et al. (2004) A proteomic analysis of human bile. *Mol Cell Proteomics* 3: 715–728.
31. Zhou H, et al. (2005) Large-scale identification of human biliary proteins from a cholesterol stone patient using a proteomic approach. *Rapid Commun Mass Spectrom* 19:3569–3578.
32. Guerrier L, et al. (2007) Contribution of solid-phase hexapeptide ligand libraries to the repertoire of human bile proteins. *J Chromatogr A* 1176:192–205.
33. Farina A, et al. (2009) Proteomic analysis of human bile from malignant biliary stenosis induced by pancreatic cancer. *J Proteome Res* 8:159–169.
34. Barbhuiya MA, et al. (2011) Comprehensive proteomic analysis of human bile. *Proteomics* 11:4443–4453.
35. Zhang D, et al. (2013) Comparative proteomic analysis of gallbladder bile proteins related to cholesterol gallstones. *PLoS One* 8:e54489.
36. Shen J, et al. (2012) Comparative proteomic profiling of human bile reveals SSP411 as a novel biomarker of cholangiocarcinoma. *PLoS One* 7:e47476.
37. Lukic N, et al. (2014) An integrated approach for comparative proteomic analysis of human bile reveals overexpressed cancer-associated proteins in malignant biliary stenosis. *Biochim Biophys Acta* 1844:1026–1033.
38. Laohaviroj M, et al. (2017) A comparative proteomic analysis of bile for biomarkers of cholangiocarcinoma. *Tumour Biol* 39:1010428317705764.
39. Rupp C, Bode KA, Leopold Y, Sauer P, Gotthardt DN (2018) Pathological features of primary sclerosing cholangitis identified by bile proteomic analysis. *Biochim Biophys Acta Mol Basis Dis* 1864:1380–1389.
40. de la Torre-Escudero E, Pérez-Sánchez R, Manzano-Román R, Oleaga A (2015) Schistosome infections induce significant changes in the host biliary proteome. *J Proteomics* 114:71–82.
41. Reichard H, Reichard P (1958) Determination of ornithine carbamyl transferase in serum. *J Lab Clin Med* 52:709–717.
42. Reichard H (1961) Ornithine carbamyl transferase activity in human serum in disease of the liver and the biliary system. *J Lab Clin Med* 57:78–87.
43. Lorentz K, Niemann E, Jaspers G, Oltmanns D (1969) Enzymes in human bile. II. Enzyme content of liver- and gallbladder bile. *Enzymol Biol Clin (Basel)* 10:528–533.
44. Reichard H (1959) Ornithine carbamyl transferase in dog serum on intravenous injection of enzyme, choledochus ligation, and carbon tetrachloride poisoning. *J Lab Clin Med* 53:417–425.
45. Kalaitzakis E, et al. (2006) Evaluation of ornithine carbamoyl transferase and other serum and liver-derived analytes in diagnosis of fatty liver and postsurgical outcome of left-displaced abomasum in dairy cows. *J Am Vet Med Assoc* 229:1463–1471.
46. Margulis L, Chapman MJ (1998) Endosymbioses: Cyclical and permanent in evolution. *Trends Microbiol* 6:342–345, discussion 345–346.
47. Alderete JS, Gaines EL, Hudson NL (1978) Contents and implications of ammonia human and canine bile. *Gastroenterology* 75:173–176.
48. Gowda GA, et al. (2006) One-step analysis of major bile components in human bile using 1H NMR spectroscopy. *Lipids* 41:577–589.
49. Zhou Z, Xu MJ, Gao B (2016) Hepatocytes: A key cell type for innate immunity. *Cell Mol Immunol* 13:301–315.
50. Antoniades CG, et al. (2012) Source and characterization of hepatic macrophages in acetaminophen-induced acute liver failure in humans. *Hepatology* 56:735–746.
51. Holt MP, Cheng L, Ju C (2008) Identification and characterization of infiltrating macrophages in acetaminophen-induced liver injury. *J Leukoc Biol* 84:1410–1421.
52. Zigmond E, et al. (2014) Infiltrating monocyte-derived macrophages and resident kupffer cells display different ontogeny and functions in acute liver injury. *J Immunol* 193:344–353.
53. Ju C, et al. (2002) Protective role of Kupffer cells in acetaminophen-induced hepatic injury in mice. *Chem Res Toxicol* 15:1504–1513.
54. You Q, et al. (2013) Role of hepatic resident and infiltrating macrophages in liver repair after acute injury. *Biochem Pharmacol* 86:836–843.
55. Thery C, Amigorena S, Raposo G, Clayton A (2006) Isolation and characterization of exosomes from cell culture supernatants and biological fluids. *Curr Protoc Cell Biol* Chapter 3:Unit 3.22.
56. Diez-Fernandez C, et al. (2013) Molecular characterization of carbamoyl-phosphate synthetase (CPS1) deficiency using human recombinant CPS1 as a key tool. *Hum Mutat* 34:1149–1159.
57. Pierson DL (1980) A rapid colorimetric assay for carbamyl phosphate synthetase I. *J Biochem Biophys Methods* 3:31–37.